New Mexico Geological Society

Downloaded from: https://nmgs.nmt.edu/publications/guidebooks/47

Hornblende-dacite pumice in the Tshirege Member of the Bandelier Tuff: Implications for magma chamber and eruptive processes

James A. Stimac

1996, pp. 269-274. https://doi.org/10.56577/FFC-47.269

in:

Jemez Mountains Region, Goff, F.; Kues, B. S.; Rogers, M. A.; McFadden, L. S.; Gardner, J. N.; [eds.], New Mexico Geological Society 47th Annual Fall Field Conference Guidebook, 484 p. https://doi.org/10.56577/FFC-47

This is one of many related papers that were included in the 1996 NMGS Fall Field Conference Guidebook.

Annual NMGS Fall Field Conference Guidebooks

Every fall since 1950, the New Mexico Geological Society (NMGS) has held an annual Fall Field Conference that explores some region of New Mexico (or surrounding states). Always well attended, these conferences provide a guidebook to participants. Besides detailed road logs, the guidebooks contain many well written, edited, and peer-reviewed geoscience papers. These books have set the national standard for geologic guidebooks and are an essential geologic reference for anyone working in or around New Mexico.

Free Downloads

NMGS has decided to make peer-reviewed papers from our Fall Field Conference guidebooks available for free download. This is in keeping with our mission of promoting interest, research, and cooperation regarding geology in New Mexico. However, guidebook sales represent a significant proportion of our operating budget. Therefore, only *research papers* are available for download. *Road logs*, *mini-papers*, and other selected content are available only in print for recent guidebooks.

Copyright Information

Publications of the New Mexico Geological Society, printed and electronic, are protected by the copyright laws of the United States. No material from the NMGS website, or printed and electronic publications, may be reprinted or redistributed without NMGS permission. Contact us for permission to reprint portions of any of our publications.

One printed copy of any materials from the NMGS website or our print and electronic publications may be made for individual use without our permission. Teachers and students may make unlimited copies for educational use. Any other use of these materials requires explicit permission.

This page is intentionally left blank to maintain order of facing pages.

HORNBLENDE-DACITE PUMICE IN THE TSHIREGE MEMBER OF THE BANDELIER TUFF: IMPLICATIONS FOR MAGMA CHAMBER AND ERUPTIVE PROCESSES

JAMES A. STIMAC

Department of Geological Sciences, University of Manitoba, Winnipeg, Manitoba, Canada R3T 2N2

Abstract—Hornblende-dacitic pumice fragments (HBDP) and their disaggregation products (streaks, wisps and xenocrysts) are common in the Tshirege (upper) Member of the Bandelier Tuff, generally comprising <1 vol% of the unit. HBDP are typically ellipsoidal in shape and have a groundmass of acicular plagioclase and hornblende set in vesicular rhyolitic glass. Coarse-grained minerals were out of equilibrium in HBDP and represent either phenocrysts that grew prior to mixing (mainly plagioclase and pyroxene), or xenocrysts derived from entrained rhyolitic magma (dominantly alkali feldspar and quartz). Groundmass minerals (mainly plagioclase and hornblende) mantle larger crystals and have textures and compositions that indicate rapid, undercooled crystallization from a limited supply of liquid. These features indicate that HBDP represent partially quenched blobs of a hybrid layer formed during addition of intermediate magma to the rhyolitic Bandelier chamber, and thus are equivalent to many quenched mafic inclusions in rhyolites and mafic microgranular enclaves in granites. Textural features of HBDP are due primarily to pre-eruptive processes, not vesiculation within the vent. HBDP are not cogenetic with the rhyolitic components of the Tshirege Member and their chemical variations are due mainly to crystal fractionation and mixing with rhyolitic magma. The presence of HBDP in the earliest erupted material suggests that addition of this magma may have destabilized the Bandelier system and triggered its eruption. This may have occurred as vesicular hybrid magma either plumed buoyantly through silicic magma, or moved more efficiently toward the vent and in the conduit system.

INTRODUCTION

Fine-grained mafic inclusions are common in silicic lavas, and are generally interpreted to result from incomplete mixing of mafic and felsic magmas (e.g., Bacon, 1986). Such inclusions in volcanic rocks are analogous to mafic microgranular enclaves described from granitic rocks, which are also thought by most workers to represent hybrid intermediate magmas formed by incomplete mixing (mingling) of silicic and mafic magmas (Didier, 1973; Eichelberger, 1980; Bacon, 1986; Vernon, 1990; Didier and Barbarin, 1991). Mafic components are also common in silicic tuffs, but have generally been described as mafic pumice or scoriae rather than mafic inclusions or enclaves because of their fragmental textures (but see Elburg, 1994). Mafic and banded pumices have generally been interpreted as representing mafic to intermediate magma layers underlying more silicic caps (Smith, 1979; Hildreth, 1981). Here, I summarize the features of hornblende-bearing dacite pumice fragments (HBDP) from the Tshirege (upper) Member of the Bandelier Tuff, and conclude that they are quenched equivalents of typical microgranular enclaves in granites. I then discuss the origin of these enclaves and what they tell us about the nature of magmatic and eruptive processes in the Bandelier magmatic system.

Previous work

The Tshirege (upper) Member of the Bandelier Tuff is one of the most studied ignimbrites in North America, and has figured prominently in the development of modern concepts of ash-flow tuff magmatism. The Tshirege Member is a compound cooling unit of some 150 km^3 dense rock equivalent (Smith and Bailey, 1966; Smith, 1979; Heiken, personal commun., 1996), erupted at 1.22 Ma (Izett and Obradovich, 1994) to form the Valles caldera. The Tshirege Member crops out throughout the Pajarito Plateau, where it is well exposed in numerous canyons (Fig. 1). Various stratigraphic nomenclatures have been devised for the Tshirege Member, generally based on the occurrence of surge beds and reversals in welding. In this study, I use the terminology of Broxton and Reneau (1995), which divides the Tshirege Member into four major subunits, with subunit 1 representing the base of the ignimbrite and subunit 4 representing its top (Fig. 2). Despite the compound nature of the unit, chemical and mineralogical variations present in the source magma appear to have been crudely preserved in vertical sections (Smith and Bailey, 1966; Smith, 1979; Balsley, 1988; Stix et al., 1988; Warshaw and Smith, 1988; Caress, 1994).

The pre-eruptive mineralogy of the Tshirege Member is complex, and appears to include contributions from at least three distinct sources (Fig. 2): (1) intratelluric grains (phenocrysts that grew "in place" from the dominant rhyolitic magma); (2) minerals included within, or derived from distinctive hornblende-dacite pumices (HBDP) and (3) minerals making

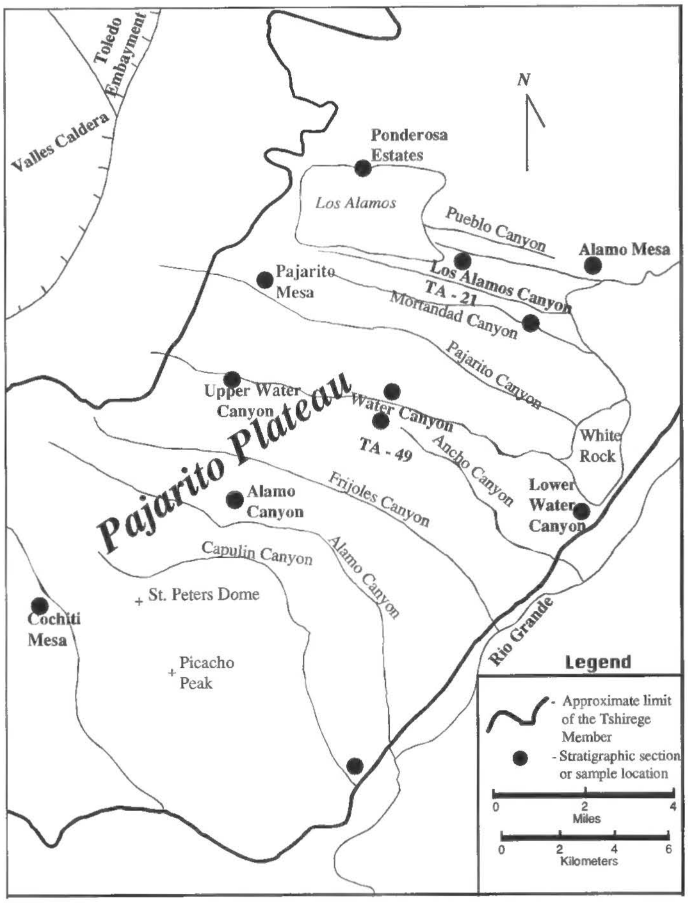

FIGURE 1. Map showing the approximate distribution of the Tshirege (upper) Member of the Bandelier Tuff on the Pajarito Plateau, Jemez Mountains, New Mexico (modified from Smith et al., 1970). Samples of HBDP are from stratigraphic sections throughout the Pajarito Plateau. Most HBDP were collected near the glassy base of the Tshirege Member (subunit 1g of Broxton and Reneau, 1995); some samples are from near contacts with paleocanyon walls or flow-tops. These areas preserve glassy pumices from subunits 2 and 3.

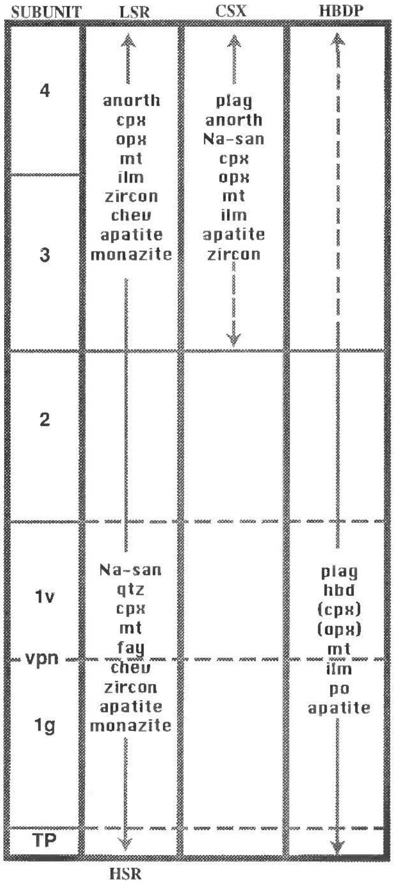

FIGURE 2. Summary of mineralogy of the major components of the Tshirege Member based on Smith and Bailey (1966), Warshaw and Smith (1988), and this study. TP is the Tsankawi Pumice Bed, and VPN is the "vapor-phase notch", which separates glassy (subunit 1g) and massively devitrified (subunits 1v, 2, 3 and 4) portions of the Tshirege Member (see Broxton and Reneau, 1995). The phenocryst assemblage of rhyolitic pumice fragments grades from sanidine (Or_{44}), quartz, clinopyroxene, fayalite, magnetite and accessory minerals in the first erupted material, to anorthoclase (Or_{25}), minor quartz, clinopyroxene, orthopyroxene, magnetite, ilmenite and accessory minerals in the last erupted material (Smith and Bailey, 1966; Warshaw and Smith, 1988; Caress, 1994). Dacitic pumices (HBDP) consist dominantly of plagioclase, clinopyroxene, orthopyroxene, hornblende, magnetite, accessory minerals and vesicular rhyolitic glass. Cognate syenitic xenoliths (CSX) consist of alkali feldspar with plagioclase cores, pyroxene, magnetite and accessory minerals, and are interpreted as lithic debris assimilated from the walls or floor of the magma body just prior to, or during eruption.

up, or derived from cognate crystal aggregates of syenitic composition (CSX), which are restricted to subunits 3 and 4 (e.g., Caress, 1994).

Bulk tuff and rhyolitic pumice fragments from the Tsankawi Pumice Bed and Tshirege Member show fairly systematic enrichment of incompatible trace elements downwards, consistent with the hypothesis that silicic magma bodies are commonly enriched in incompatible trace elements towards their tops, and that ash-flow tuffs variably preserve an inverted version of this zonation (e.g., Smith, 1979; Hildreth, 1981). The observed chemical variations in the Tshirege Member appear to result mainly from crystal fractionation; however, as with the Otowi Member (see Dunbar and Hervig, 1992), mixing of high-Sr and low-Sr compositions is also indicated (Balsley, 1988; Stimac and Budahn, unpub. data). As discussed later, this may be due to the mixing of distinctive rhyolitic components, or to mixing of rhyolite with HBDP magma. Assimilation of syenitic lithic debris adds additional chemical heterogeneity in subunits 3 and 4.

Several workers have noted that HBDP bear mineralogical and chemical similarities to earlier-erupted Tschicoma and Cerro Rubio dacites, but do not appear to be genetically related to the dominant rhyolitic component of the Tshirege Member (Smith and Bailey, 1966; Balsley, 1988; Stix et al., 1988). Smith (1979) suggested that a large reservoir of latitic magma similar in composition to HBDP existed beneath the rhyolitic portion of the Bandelier magma chamber prior to eruption, and implied that the HBDP may be samples of this "dominant volume". He envisioned that this latitic layer was underlain by basaltic magma.

Little work on the mineralogy and textures of dacitic pumices has been published. Balsley (1988) interpreted the large sieve-textured feldspars they contain as the products of rapid growth during undercooled crystallization. In this paper I document the mineralogy and textures of HBDP in more detail, and speculate on their origin and implications for magma chamber processes just prior to eruption of the Tshirege Member.

OBSERVATIONS

Hornblende dacite enclaves

Dacitic hornblende-bearing pumices (HBDP) were sampled from several localities throughout the Pajarito Plateau (Fig. 1; Table 1). HBDP apparently are present throughout the Tshirege Member, comprising from <1 to 10% of the unit (Smith and Bailey, 1966; Balsley, 1988). My observations suggest that HBDP generally comprise <1 vol% of outcrops, and are most abundant in the earlier erupted material. In fact, HBDP appear to be absent in many outcrops of subunits 3 and 4, but more detailed study is needed to confirm this (Fig. 2). HBDP are ellipsoidal in shape and range in size from <1 to 30 cm, but most are <10 cm in long dimension. Individual HBDP clasts commonly have both angular and rounded surfaces. All examined samples exhibit stretching fabrics parallel to their long dimension, including large tubular vesicules (up to several cm in length) and trains of large crystal fragments connected by spindle glass (up to 3 cm in length). Pumice margins are commonly crenulate or ribbed parallel to their long dimension.

HBDP are light gray to dark gray and porous due to abundant tiny (<1 mm) vesicles. Small HBDP show no core-to-rim variation in grain size or vesicularity, but some larger HBDP (e.g., MORT1; see Table 1) have fine-grained, non-vesicular rims and coarser-grained, vesicular cores, with the coarse-vesicular texture extending to flat, broken surfaces. This suggests that internal crystallization and vapor exsolution occurred prior to brittle fracturing, possibly accompanied by gas filter pressing (cf., Bacon, 1986). Some HBDP are weakly banded in shades of light to dark gray due to variations in hornblende content. One pumice sample contains streaks of nearly hornblende-free silicic glass with large, nearly pristine quartz and alkali feldspar. The hornblende-bearing portion of this pumice contains partially reacted grains of these minerals. It is likely that this pumice preserves two distinct magmatic components, including the silicic component from the original site of hybridization at or near the base of the rhyolitic portion of the magma body, but more work is needed to confirm this.

HBDP have a fine-grained, porphyritic texture, with the larger crystals easily divided into two types, early-formed phenocrysts and reacted xenocrysts. Early-formed phenocrysts (generally several mm long) are plagioclase, clinopyroxene and orthopyroxene ± magnetite. These grains commonly form crystal aggregates mantled by hornblende ± magnetite and typically comprise <5 vol% of pumices. HBDP also contain <3 to 10 vol% large (up to 1 cm across), fractured, sieve-textured alkali feldspar and resorbed quartz (generally several mm across) similar in size to phenocrysts in rhyolitic pumices. Most feldspar grains are completely reacted to sieve-textured plagioclase, but rare examples contain unreacted alkali feldspar cores. These textures confirm that plagioclase formed by reactions that progressed inward from crystal margins rather than by rapid outward growth as suggested by Balsley (1988). In some HBDP, quartz grains are mantled by fine-grained plagioclase or hornblende, forming a corona texture. Similar fine-grained holocrystalline aggregates of plagioclase and hornblende up to 1 cm across are distributed throughout the glassy matrix of some pumices, but their origin is unclear.

The matrix of HBDP consists of fine-grained (generally <1 mm) equant to acicular plagioclase, hornblende (up to 3 mm in long dimension), magnetite, ilmenite, apatite and pyrrhotite set in vesicular rhyolitic glass. In some HBDP biotite and alkali feldspar mantle earlier-formed hornblende and plagioclase, or partially fill vesicles; however, biotite is only abundant in partially or completely devitrified samples.

In addition to forming discrete pumices, plagioclase and hornblende-bearing streaks and wisps are present within some rhyolitic pumices.

TABLE 1. Whole-rock chemical data for hornblende-dacitic pumices from the Tshirege Member.

Sample	MORT1A	MORT1B	TA-49	HBP-1	F82-95	27-25i	27-26ai	22-69a	22-70
XRF DATA									
SiO2	65.88	66.01	65.89	66.38	67.40	66.92	67.04	67.93	67.51
TiO2	0.44	0.46	0.47	0.40	0.43	0.41	0.41	0.40	0.414
Al2O3	14.77	14.91	15.36	14.32	15.00	14.64	14.41	14.54	14.74
Fe2O3	3.60	3.66	3.72	3.28	3.20	3.31	3.24	3.35	3.35
MnO	0.08	0.07	0.06	0.07	0.06	0.07	0.08	0.07	0.07
MgO	1.34	1.35	1.39	1.13	1.35	1.37	1.26	1.29	1.34
CaO	3.12	3.22	3.43	3.41	3.19	3.22	2.98	2.95	2.94
Na2O	4.34	4.39	4.01	4.50	4.86	4.17	4.66	4.79	4.78
K2O	3.86	3.56	3.24	3.28	2.85	3.49	3.67	3.06	3.24
P2O5	0.17	0.17	0.17	0.15	0.16	0.15	0.15	0.15	0.152
LOI	1.20	1.15	1.57	2.26	1.42	2.52	1.83	1.46	1.28
TOTAL	97.60	97.79	97.75	96.91	99.92	100.26	99.72	99.99	99.82
Rb	183	177	157	165	151	79	167	151	178
Sr	456	488	540	384	514	411	391	442	433
Y	24	24	20	22	31	26	28	35	26
Zr	187	194	173	221	229	235	214	202	211
Nb	29	23	17	18	32	23	28	38	27
V	50	48	49	41	nd	nd	nd	nd	nd
Cr	25	26	23	21	nd	nd	nd	nd	nd
Ni	20	17	20	14	nd	nd	nd	nd	nd
Zn	84	70	72	62	nd	nd	nd	nd	nd
Ba	885	1012	1098	852	nd	950	778	969	902
INAA DATA									
Sc	nd	nd	nd	nd	nd	nd	5.56	5.52	5.74
Cr	nd	nd	nd	nd	nd	nd	18.5	20	19.3
Co	nd	nd	nd	nd	nd	nd	nd	nd	nd
Zn	nd	nd	nd	nd	nd	nd	nd	nd	nd
As	nd	nd	nd	nd	nd	nd	15.7	nd	nd
Rb	nd	nd	nd	nd	nd	nd	160	145	171
Sb	nd	nd	nd	nd	nd	nd	0.08	0.13	0.12
Cs	nd	nd	nd	nd	4	nd	4.4	4.6	3.9
Ba	nd	nd	nd	nd	nd	nd	778	936	922
Zr	nd	nd	nd	nd	nd	nd	nd	nd	nd
Hf	nd	nd	nd	nd	6.6	nd	5.9	6.42	6.28
Ta	nd	nd	nd	nd	nd	nd	2.2	3.3	2
Th	nd	nd	nd	nd	11	nd	7.8	10	7.7
U	nd	nd	nd	nd	2.7	nd	2.7	3.2	2.2
La	nd	nd	nd	nd	37	nd	38.1	36	37
Ce	nd	nd	nd	nd	79	nd	74.2	70.4	69.4
Nd	nd	nd	nd	nd	38	nd	25.4	25.7	25.8
Sm	nd	nd	nd	nd	5.3	nd	5.3	5.4	5.1
Eu	nd	nd	nd	nd	0.9	nd	0.816	0.846	0.879
Gd	nd	nd	nd	nd	nd	nd	nd	nd	nd
Tb	nd	nd	nd	nd	nd	nd	0.76	0.88	0.71
Yb	nd	nd	nd	nd	3	nd	2.47	3.05	2.36
Lu	nd	nd	nd	nd	0.42	nd	0.37	0.47	0.37

MORT1A and B are the rim and core of a large HBDP. Samples MORT1A and B from Mortandad Canyon; TA-49 from Water Canyon; HBP-1 from Los Alamos Canyon.
Samples 27-25i and 27-26ai (Pueblo Mesa), and 22-69a and 22-70 (Otowi Mesa) from Balsley, 1988.
Sample F82-95 from Stix et al., 1988.
XRF, X-ray fluorescence; INAA, instrumental neutron activation analysis; nd, not determined.
Total Fe as Fe2O3.

Moreover, hornblende, plagioclase and pyroxene xenocrysts similar in composition and texture to minerals comprising HBDP are disseminated throughout the Tshirege Member in trace abundances. Some of these xenocrysts are partially enclosed in fine-grained matrix material, confirming that they were derived from disaggregation of HBDP.

Mineral compositions of hornblende-dacite pumices

Warshaw and Smith (1988) and Caress (1994) documented systematic variations in the compositions of phenocrysts in the Tshirege Member. These studies focussed on phenocryst compositions in rhyolitic pumices, but recognized the presence of xenocrysts derived from other sources. Electron microprobe data for feldspar and pyroxene in HBDP are summarized in Figure 3 and Tables 2 and 3. Plagioclase forming aggregates with pyroxene and hornblende ranges in composition from An_{15} to An_{52}, with the most calcic compositions occurring outboard of ragged dissolution surfaces (filled triangles in Fig. 3). These "calcic spikes" are most common near crystal margins, and show a relatively restricted compositional range from An_{46} to An_{52}. Groundmass plagioclase has a wide range in grain size (<0.1 to 2 mm), is normally zoned, and ranges from An_{21} to An_{54}. Plagioclase mantles on quartz xenocrysts show a more restricted compositional range (open circles), overlapping with groundmass and phenocryst compositions. Large alkali feldspar xenocrysts have unreacted cores ranging in composition from Or_{28} to Or_{36} (open squares). This range is similar to that observed in subunits 2 and 3 of the Tshirege Member. Reacted regions mantling these preserved cores (filled squares) have a sieved texture consisting of intergrown plagioclase and glass with compositions between groundmass plagioclase and unreacted alkali feldspar cores. Thin alkali feldspar mantles on plagioclase range in composition from Or_{25} to Or_{46} (open circles), or to more potassic compositions than alkali feldspar phenocrysts in the host rhyolite, which are only as potassic as Or_{44}.

Early-formed pyroxene forming aggregates with plagioclase are considerably more Mg-rich than the dominant pyroxene compositions in the Tshirege Member, but overlap in composition with phenocrysts from the last-erupted material (Warshaw and Smith, 1988; Fig. 3B). Orthopyroxenes in HBDP range to more Mg-rich compositions than Tshirege phenocrysts, whereas clinopyroxene in HBDP overlaps in composition with phenocrysts thought to be from subunits 2 and 3 (Warshaw and Smith, 1988). Textural relations indicate that pyroxene grains in HBDP acted as nucleation sites for hornblende ± magnetite, which grew during undercooled crystallization of HBDP groundmass minerals.

Whole-rock chemical data for hornblende-dacite pumice

Whole-rock chemical data for the Tsankawi Pumice Bed and Tshirege Member of the Bandelier Tuff, including data for HBDP, were compiled

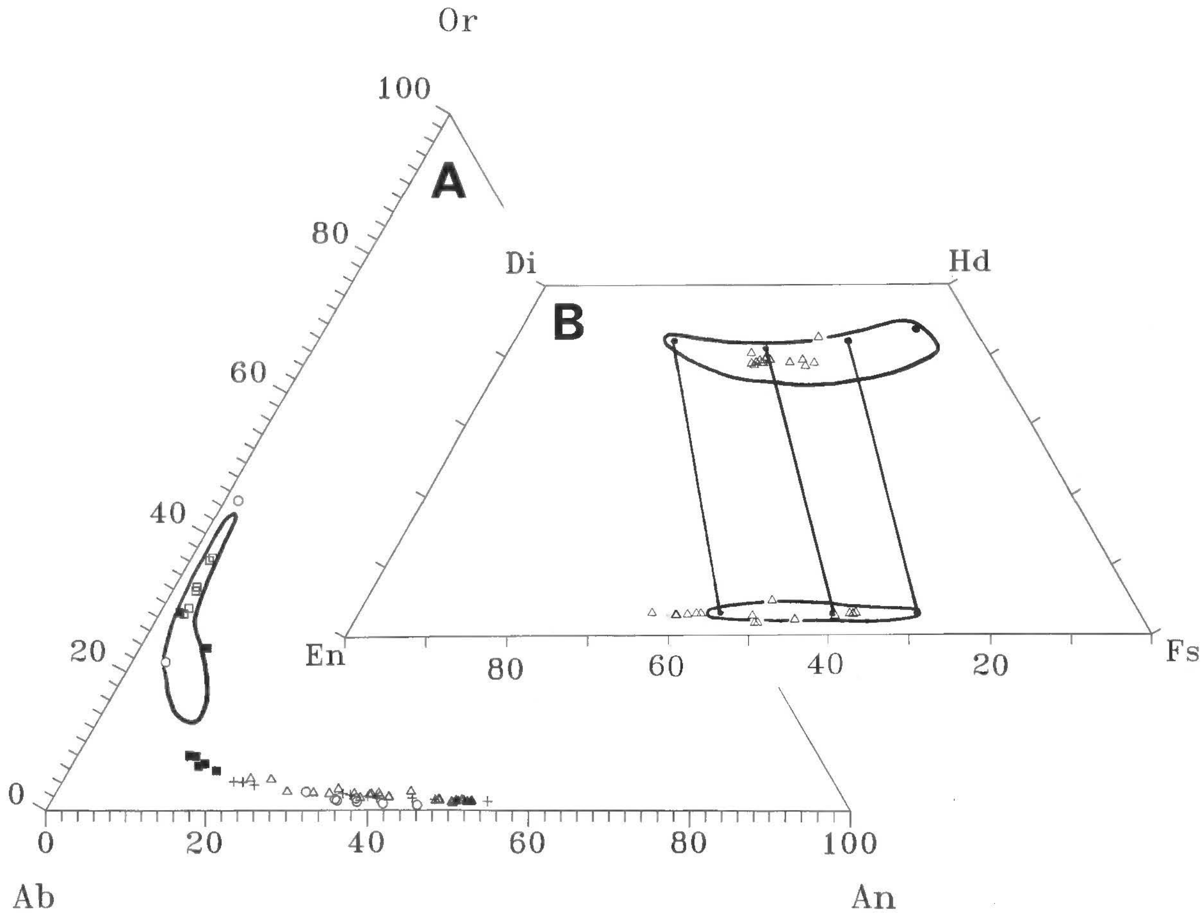

FIGURE 3. Electron microprobe data for feldspar and pyroxene in HBDP (mol%). Circled fields show the approximate ranges of feldspar and pyroxene phenocryst compositions determined for the Tshirege Member by Caress (1994), Warshaw and Smith (1988) and this study. A, Plagioclase grains in aggregates with pyroxene and hornblende (open and filled triangles); groundmass plagioclase (crosses); mantles (open circles); unreacted alkali feldspar cores (open squares); sieve-textured reaction products of alkali feldspar rims (filled squares). B, Pyroxene grains in aggregates with plagioclase (open triangles). Solid circles connected by tielines are phenocryst compositions from the Tshirege Member (Warshaw and Smith, 1988).

from various sources (Balsley, 1988; Stix et al., 1988; Broxton et al., 1995; Stimac et al., in press; Gardner, unpub. data). The compositions of bulk tuff samples and rhyolitic pumice fragments overlap and show moderately good correlation with stratigraphic position. This is best seen in variation diagrams where two highly incompatible elements such as Rb and Nb are plotted; such elements typically define linear trends, with the slope being a measure of relative incompatibility (Fig. 4A). Sampling of bulk tuff from subunits 3 and 4 greatly extend the chemical variations in the Tshirege Member documented by Balsley (1988), who restricted his attention to glassy pumices representing subunits 1 and 2. HBDP are dacitic but show a range in major and trace element composition (Fig. 4), with variations correlated with the abundance of xenocrystic anorthoclase and quartz. HBDP do not show any systematic relationship to rhyolitic pumices of the Tshirege Member, either in terms of mineralogy or chemistry, suggesting that they are not genetically related to the bulk of the Bandelier rhyolitic magma (Balsley, 1988; Stix et al., 1988). Variable incorporation of HBDP magma or crystalline debris into the zoned rhyolitic magma likely is responsible for outrange variations of Sr, Ba, Ca and Ti in some rhyolitic pumices. Figure 4B shows that pumice fragment and bulk-tuff samples with relatively high Sr compared to the main data trend could be explained by mixing of a small amount of HBDP magma into the existing zoned rhyolitic magma. This could be the result of mingling at the scale of individual pumices and bulk-tuff samples, and/or entrainment of HBDP magma debris.

As noted by earlier workers, HBDP bear mineralogical and chemical similarities to Cerro Rubio and Tschicoma dacites (Smith and Bailey, 1966; Balsley, 1988; Stix et al., 1988), and are the approximate composition of magma presumed to be parental to rhyolitic Bandelier magma by Smith (1979). Moreover some Cerro Toledo tephras contain plagioclase and hornblende (Stix and Gorton, 1990), and have high Ti, Al, Mg, Ca, Sr and Ba. Although disequilibrium textures have not been described from Cerro Toledo rocks, the presence of plagioclase and hornblende may indicate that formation of hybrid magma like the HBDP was not an isolated event, but occurred repeatedly during the Bandelier magmatic cycles.

DISCUSSION AND CONCLUSIONS

HBDP from the Tshirege Member of the Bandelier Tuff share many features with quenched inclusions from silicic lavas including (1) ellipsoidal shape; (2) fine-grained groundmass consisting of acicular, normally zoned minerals in a vesicular glassy matrix; (3) partially reacted xenocrysts derived from a more silicic magma; and (4) phenocrysts that appear to have formed in a precursor, more mafic magma (cf., Eichelberger, 1980; Bacon, 1986; Stimac et al., 1990; Vernon, 1990). Based on the presence of fine-grained chilled margins on some large HBDP, brittle fracture of some margins, and alkali feldspar xenocrysts with compositions similar to later erupted subunits of the Tshirege Member, it seems likely that some, if not all, of these HBDP were discrete enclaves *prior to* fragmentation of the bulk magma, and therefore are not pumices in the strict sense. Moreover, all these features are consistent with an origin by mixing of a more mafic (andesitic?) magma with alkali feldspar- and quartz-bearing rhyolitic magma similar to subunits 2-3 in the lower portions of the rhyolitic magmatic system. This hybrid dacitic magma may have formed a discrete layer, which eventually was entrained in the overlying rhyolite directly preceding or during eruption, forming the HBDP by partial quenching. The most calcic plagioclase crystals forming aggregates with Mg-rich pyroxene in HBDP may have begun crystallization prior to or during hybridization, whereas hornblende and more sodic plagioclase appear to have grown largely during undercooled

TABLE 2. Selected electron microprobe data for feldspar in HBDP.

Sample	SiO2	Al2O3	FeO	CaO	Na2O	K2O	BaO	Total	Ab	Or	An	Cs	iv	vi	iv+vi
af xc/ur	66.23	19.13	0.23	0.51	6.90	6.17	nd	99.16	61.41	36.11	2.48	nd	3.998	0.981	4.979
af xc/ur	67.90	19.07	0.14	0.65	7.94	5.01	0.11	100.81	68.38	28.35	3.09	0.18	3.989	0.995	4.984
af xc/ur	67.49	18.98	0.19	0.60	7.52	5.55	0.05	100.38	65.31	31.71	2.89	0.09	3.990	0.991	4.981
af xc/r	69.38	18.97	0.16	2.81	7.18	0.97	nd	99.46	76.61	6.80	16.59	nd	4.010	0.795	4.805
af xc/r	80.33	11.46	0.19	0.30	4.79	3.02	nd	100.09	68.97	28.64	2.40	nd	3.994	0.573	4.567
af xc/r	70.55	17.57	0.17	2.34	6.67	1.03	nd	98.33	77.16	7.87	14.98	nd	4.013	0.736	4.749
af m pl	66.04	18.97	0.18	0.53	7.40	5.29	0.34	98.74	65.83	30.94	2.62	0.61	3.995	0.985	4.980
af m pl	66.13	18.75	0.16	0.25	6.79	6.48	nd	98.56	60.69	38.09	1.23	nd	3.998	0.984	4.982
af m pl	67.02	19.15	0.15	0.21	6.63	7.23	nd	100.39	57.62	41.35	1.03	nd	3.997	0.995	4.992
pl m qtz	56.94	26.63	0.28	9.15	6.06	0.30	0.05	99.42	53.51	1.74	44.65	0.10	3.990	0.992	4.982
pl gm	53.57	28.33	0.46	11.09	5.02	0.23	0.07	98.77	44.39	1.33	54.15	0.12	3.986	1.005	4.991
pl gm	61.51	23.24	0.30	5.01	8.21	0.63	0.14	99.04	71.92	3.61	24.23	0.25	3.992	0.994	4.986
pl gm	57.83	25.83	0.39	8.07	6.73	0.35	0.10	99.30	58.85	1.99	38.98	0.18	3.988	1.003	4.991
pl c-s	54.33	28.03	0.40	10.59	5.38	0.26	nd	99.00	47.16	1.50	51.34	nd	3.986	1.009	4.995
pl c-s	54.67	28.47	0.37	10.78	5.26	0.24	nd	99.79	46.24	1.40	52.35	nd	3.991	0.997	4.988
pl pr	59.11	25.06	0.16	6.99	7.34	0.45	0.02	99.12	63.80	2.57	33.60	0.03	3.994	1.005	4.999
pl pr	61.77	23.42	0.19	5.29	8.14	0.81	0.11	99.72	70.09	4.57	25.15	0.19	3.989	1.006	4.995
pl pr	63.48	21.25	0.18	3.42	8.81	1.36	0.15	98.65	75.77	7.70	16.26	0.27	3.983	1.015	4.998
pl pz	62.85	22.43	0.16	4.09	8.42	1.09	0.09	99.13	73.76	6.28	19.80	0.16	3.996	0.990	4.986
pl pz	60.74	24.03	0.16	6.09	8.01	0.52	0.05	99.61	68.31	2.91	28.70	0.08	3.987	1.018	5.005
pl pz	55.30	27.59	0.38	10.01	5.77	0.29	nd	99.34	50.24	1.65	48.11	nd	3.986	1.012	4.998
pl pz	56.61	26.64	0.30	8.72	6.50	0.37	nd	99.13	56.24	2.09	41.68	nd	3.990	1.015	5.005
pl pc	55.71	27.19	0.33	9.86	5.71	0.28	0.03	99.09	50.34	1.59	48.01	0.06	3.988	1.000	4.988
pl pc	54.94	27.41	0.34	10.40	5.51	0.27	0.05	98.92	48.12	1.57	50.22	0.09	3.981	1.012	4.993
pl pc	58.50	25.74	0.18	7.53	6.78	0.43	nd	99.18	60.40	2.54	37.07	nd	4.002	0.981	4.983
pl pc	54.97	28.42	0.44	10.80	5.30	0.25	nd	100.18	46.34	1.46	52.20	nd	3.988	1.000	4.988

Abbreviations: pl, plagioclase; af, alkali feldspar; xc/ur, unreacted xenocryst; xc/r, reacted xenocryst; pc, phenocryst; pr, phenocryst rim; pz, internal zone; m, mantle; cs, calcic spike.
iv, Si+Al; vi, Ca+Na+K+Ba.
nd, not determined.

crystallization attending mixing. HBDP do not preserve direct evidence of basaltic injection into the Bandelier system, but the most calcic zones in larger plagioclase crystals may record the thermal and compositional effects of basaltic incursions at deeper levels.

Mechanical disaggregation of HBDP occurred during entrainment in rhyolitic magma, when the viscosities of the HBDP and host magma were similar, and continued to final eruption and emplacement. The HBDP magma was originally at higher temperature and was more mafic than the overlying rhyolite, and was therefore lower in viscosity. However, upon rapid cooling and crystallization, its viscosity eventually increased and became similar to the overlying rhyolite (Sparks and Marshall, 1986). It is at this stage that disaggregation likely became an important process, as has been documented for quenched mafic inclusions in lavas (Stimac and Pearce, 1992). Volatile saturation and vesiculation also would accompany crystallization, and potentially produced buoyancy in the HBDP magma (e.g., Eichelberger, 1980). Large tubular vesicles and the elongate shape of HBDP may indicate rapid upward expansion due to simultaneous flow and vesiculation. Smith (1979) noted that it is common for mafic magma to form discrete pumices in ignimbrites, and that these "pumices" are commonly chilled against the silicic magma, indicating that they formed discrete lumps *prior to* eruption.

Smith (1979) suggested that the Bandelier magma chamber consisted of a rhyolitic cap, a "dominant volume" latitic zone, and a deep basaltic zone. He implied a large reservoir of HBDP magma existed beneath the rhyolitic portion of the Bandelier magma chamber prior to eruption, but noted that its thickness probably varied as a function of rates of rhyolitic eruption and basaltic influx into the base of the system. Textures of HBDP indicate that they formed via incomplete mixing of andesitic(?) magma and rhyolitic magma just prior to eruption of the Tshirege Member. Therefore they do not represent a "dominant volume" layer of long-lived dacitic magma beneath the rhyolitic system, but rather a transient layer, probably formed by more mafic intrusion at depth.

Chemical zonation of the Tshirege member is largely explained by crystal fractionation, mixing of discrete high-Sr and low-Sr magmas, and disaggregation of HBDP and syenitic lithic debris. It appears that HBDP are not parental to either rhyolitic magma type (Balsley, 1988) but may have a closer affinity to low-Si pumices high in Sr, Ba, Ti and Ca, but further study is needed to confirm this.

TABLE 3. Selected electron microprobe data for pyroxenes in HBDP.

Sample	SiO2	TiO2	Al2O3	FeO	MnO	Na2O	MgO	CaO	ZnO	Fe2O3	Total	Wo	En	Fs	iv	vi	iv+vi
pz	52.14	0.35	1.21	23.59	1.02	0.06	20.05	1.51	0.11	0.25	100.28	3.11	57.37	39.52	2.016	1.966	3.982
pz	51.80	0.37	1.17	23.40	0.94	0.05	20.01	1.49	0.13	0.46	99.82	3.09	57.58	39.33	2.011	1.966	3.977
pz	52.51	0.41	1.44	21.98	0.82	0.03	21.24	1.69	0.09	0.00	100.20	3.45	60.24	36.31	2.022	1.965	3.987
pz	51.52	0.34	1.19	24.70	1.06	0.06	18.92	1.59	0.10	0.80	100.28	3.31	54.82	41.87	2.008	1.961	3.969
pz	51.95	0.26	0.84	24.50	0.89	0.03	19.56	1.54	0.00	0.03	99.58	3.18	56.02	40.80	2.011	1.981	3.992
pz	50.65	0.38	1.20	28.49	1.40	0.20	14.77	2.41	0.03	0.00	99.52	5.20	44.37	50.43	2.031	1.950	3.981
pz	50.73	0.22	0.97	28.33	1.28	0.05	16.28	1.41	0.23	0.52	100.02	3.00	47.99	49.01	2.009	1.968	3.977
pz	49.94	0.26	0.54	33.51	1.76	0.04	12.53	1.35	0.12	0.00	100.06	2.92	37.62	59.46	2.009	1.980	3.989
pz	51.88	0.12	0.48	17.56	1.21	0.48	9.74	18.17	0.00	0.00	99.63	39.17	29.22	31.61	2.031	1.961	3.992
pz	51.72	0.14	0.52	17.30	1.26	0.46	10.05	18.22	0.00	0.38	100.06	39.02	29.94	31.05	2.019	1.964	3.983
pz	51.18	0.20	0.48	17.90	1.25	0.45	9.53	18.09	0.00	0.39	99.44	39.07	28.63	32.31	2.016	1.966	3.982
pz	51.19	0.16	0.46	17.98	1.28	0.46	9.42	18.06	0.05	0.58	99.63	39.09	28.36	32.56	2.015	1.963	3.978

Abbreviations same as in Table 2.
iv, Si+Al; vi, Fe2+Mn+Mg+Ca+Zn.

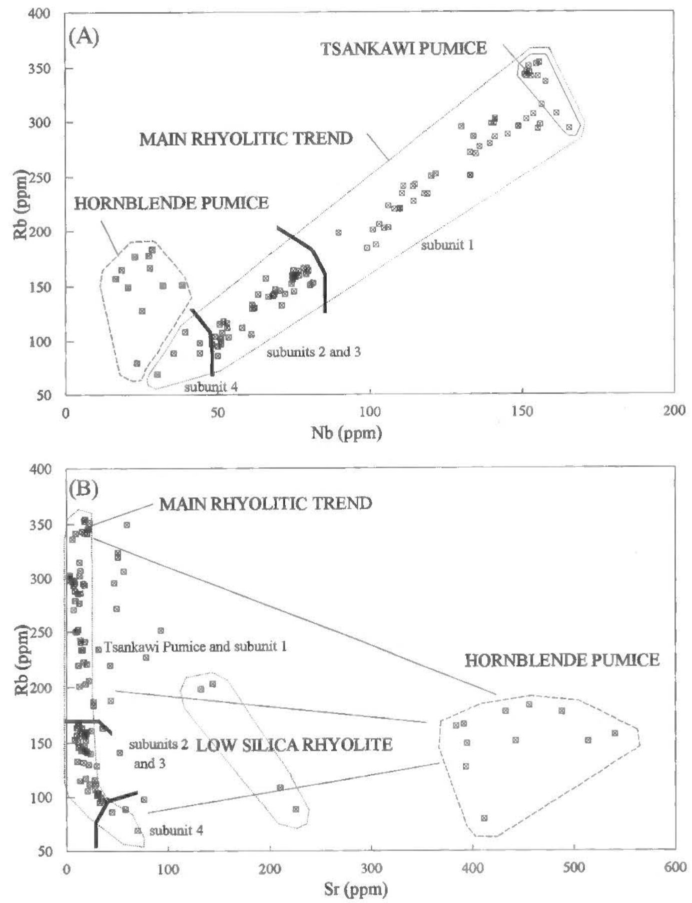

FIGURE 4. Plots of whole-rock analyses of bulk-tuff, and rhyolitic and dacitic pumices from the Tshirege Member. A, Rb versus Nb. Fields of HBDP, the main rhyolite trend, and the Tsankawi Pumice Bed are shown for reference. The approximate fields of samples from subunits 1 (first erupted) to 4 (last erupted) are also separated by heavy dividing lines. B, Sr versus Rb. Fields same as in Figure 4A. Thin solid lines are possible mixing arrays between rhyolitic and HBDP components, and may explain outrange rhyolite data with high Sr concentrations.

The preservation of incomplete magma mixing and reaction of xenocrysts, and acicular groundmass minerals set in rhyolitic glass all indicate that HBDP formed just prior to eruption of the Tshirege Member. It therefore seems likely that new intrusion of intermediate or mafic magma into the Bandelier magma body may have triggered eruption. The presence of HBDP enclaves throughout the Tshirege Member implies that this component of the eruption was able to reach the vent during the earliest stages of eruption (Blake and Ivey, 1986). Recent simulations of intrusion of hot mafic magma at the base of more silicic magma suggest that plumes of the hotter mafic component can become buoyant by volatile saturation and viscous coupling, and intrude higher levels of the system prior to or during withdrawal from above. It is not known whether such plumes could penetrate relatively viscous rhyolitic magma, but new models for transport of metals in magmatic systems suggest that buoyant permeable foams may be relatively common in silicic magmatic systems (e.g., Candela, 1992).

ACKNOWLEDGMENTS

Much of this study was completed while the author was a Director's-funded Postdoctoral fellow at Los Alamos National Laboratory. Additional support came from an LDRD grant to D. Hickmott. I am especially thankful for the generosity of Fraser Goff, Dave Broxton, Ken Wohletz and Don Hickmott during my time at Los Alamos National Lab. Numerous discussions with them, as well as Jamie Gardner, John Wolff, Grant Heiken and Mary Caress greatly contributed to my understanding of the Bandelier magmatic system. Dave Broxton and Grant Heiken also provided helpful and timely reviews of this manuscript. Thanks also to David Sawyer and Jim Budahn of the U.S. Geological Survey, who provided instrumental neutron activation data on selected Bandelier Tuff samples. Additional help came from Emily Kluk, who performed the XRF analyses, Dave Mann who made thin sections, and Peggy Snow who helped with microprobe work.

REFERENCES

Bacon, C. R., 1986, Magmatic inclusions in silicic and intermediate volcanic rocks: Journal of Geophysical Research. v. 91, p. 6091-6112.

Balsley, S. D., 1988, The petrology and geochemistry of the Tshirege member of the Bandelier Tuff, Jemez Mountains volcanic field, New Mexico, USA [MS thesis]: Arlington, University of Texas, 188 p.

Blake, S. and Ivey, G. N., 1986, Density and viscosity gradients in zoned magma chambers, and their influence on withdrawal mechanics: Journal of Volcanology and Geothermal Research., v. 30, p. 201-230.

Broxton, D. E. and Reneau, S. L., 1995, Stratigraphic nomenclature of the Bandelier Tuff for the Environmental Restoration Project at Los Alamos National Laboratory: LANL Report LA-13010-MS, 21 p.

Broxton, D. E., Heiken, G., Chipera, S. J. and Byers, F. M., Jr., 1995, Stratigraphy, petrography, and mineralogy of tuffs at Technical area 21, Los Alamos National Laboratory, New Mexico: LANL Report LA-12934-MS; 31 p.

Candela, P. A., 1992, Controls on ore metal ratios in granite-related ore systems: an experimental and computational approach: Transactions of the Royal Society of Edinburgh, Earth Sciences, v. 83, p. 317-326.

Caress, M., 1994, Feldspar compositions from the Bandelier Tuff, New Mexico: insights into magma chamber processes: Eos, v. 75(44), p. 748-749.

Didier, J., 1973, Granites and their enclaves: the bearing of enclaves on the origin of granites: Developments in Petrology, v. 3, Amsterdam, Elsevier, 393 p.

Didier, J. and Barbarin, B., 1991, The different types of enclaves in granites—nomenclature; *in* Didier, J. and Barbarin, B., eds., Enclaves and granite petrology: Developments in Petrology, v. 13, Amsterdam, Elsevier, 19-23 p.

Dunbar, N. W. and Hervig, R. L., 1992, Volatile and trace element composition of melt inclusions from the lower Bandelier Tuff: implications for magma chamber processes and eruptive style: Journal of Geophysical Research, v. 97, p. 15151-15170.

Eichelberger, J. C., 1980, Vesiculation of mafic magma during replenishment of silicic magma reservoirs: Nature, v. 288, p. 446-450.

Elburg, M. A., 1994, The origin of mafic microgranular enclaves in an S-type ignimbrite: Eos, v. 75, p. 751.

Hildreth, W., 1981, Gradients in silicic magma chambers: implications for lithospheric magmatism: Journal of Geophysical Research, v. 86 p. 10,153-10,192.

Izett, G. A. and Obradovich, J. D., 1994, $^{40}Ar/^{39}Ar$ age constraints for the Jaramillo Normal Subchron and the Matuyama-Brunhes geomagnetic boundary: Journal of Geophysical Research, v. 99, p. 2925-2934.

Smith, R. L. and Bailey, R. A., 1966, The Bandelier Tuff: a study of ash-flow eruption cycles and zoned magma chambers: Bulletin Volcanologique, v. 29, p. 83-104.

Smith, R. L., 1979, Ash-flow magmatism: Geological Society of America, Special Paper 180, p. 5-28.

Sparks, R. S. J. and Marshall, L. A., 1986, Thermal and mechanical constraints on mixing between mafic and silicic magmas: Journal of Volcanology and Geothermal Research, v. 29, p. 99-124.

Stimac, J. A. and Pearce, T. H., 1992, Textural evidence of mafic-felsic magma interaction in dacitic lavas, Clear Lake, California: American Mineralogist, v. 77, p. 795-809.

Stimac, J. A., Hickmott, D., Abell, R., Larocque, A. C. L., Broxton, D., Gardner, J., Chipera, S., Wolff, J. and Gauerke, E. (in press), Redistribution of Pb and other volatile trace metals during eruption, devitrification, and vapor-phase crystallization of the Bandelier Tuff, New Mexico: Journal of Volcanology and Geothermal Research.

Stimac, J. A., Pearce, T. H., Donnelly-Nolan, J. M. and Hearn, B. C., 1990, Origin and implications of undercooled andesitic inclusions in rhyolites, Clear Lake, California: Journal of Geophysical Research, v. 95, p. 17729-17746.

Stix, J. and Gorton, M. P., 1990, Changes in silicic melt structure between the two Bandelier caldera-forming eruptions, New Mexico, USA: evidence from zirconium and light rare earth elements: Journal of Petrology, v. 31, p. 1261-1283.

Stix, J., Goff, F., Gorton, M. P, Heiken, G. and Garcia, S., 1988, Restoration of compositional zonation in the Bandelier silicic magma chamber between two caldera-forming eruptions: geochemistry and origin of the Cerro Toledo Rhyolite, Jemez Mountains, New Mexico: Journal of Geophysical Research, v. 93, p. 6129-6147.

Vernon, R. H., 1990, Crystallization and hybridism in microgranitoid enclave magmas: microstructural evidence: Journal of Geophysical Research, v. 95, p. 17849-17859.

Warshaw, C. M. and Smith, R. L., 1988, Pyroxenes and fayalites in the Bandelier Tuff, New Mexico: temperatures and comparison with other rhyolites: American Mineralogist, v. 73, p. 1025-1037.